Biological Fidelity

Structural & **Functional**

Validations

Validation Level

Level 1 Directly Parameterized	We explicitly set this in our algorithms.
Level 2 Fitted	We do not explicitly set this, but we optimize other parameters to obtain this.
Level 3 Emerging Locally	We did not try to achieve this, but it emerges because we model the underlying processes correctly.
Level 4 Emerging Distally	Similar to 3, but the phenomenon is further removed from the underlying parameters.
Level 5 Emerging Prediction	This is a phenomenon that had not been known until we characterized it in the model. It has subsequently been validated in experimental data.

Biological Comparison - Structural and Functional Validations

I. **Structural validations - small to large scale**
   - A. **Subcellular**
   - B. **Pairwise**
   - C. **Population**
   - D. **Network**

II. Functional validations - small to large scale
   - A. Single cell
   - B. Paired cells
   - C. Population

III. References

I. Subcellular - Validation of **bouton densities**

Level 1 | Level 2 | Level 3 | Level 4 | Level 5

This validates to what degree we match the overall number of outgoing synapses a neuron forms.

Our techniques keep improving and allow successively better fits.

2015 rat model

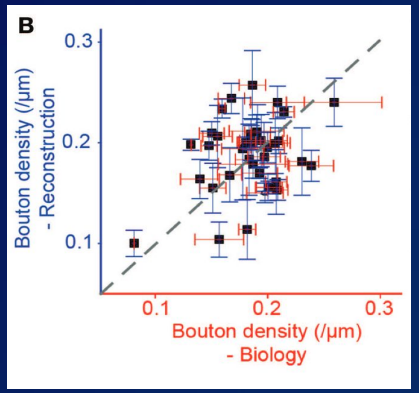

Reimann et al., 2015

2023 rat model

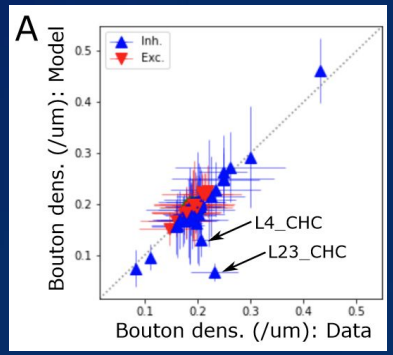

Reimann et al., 2023

2023 thalamus model

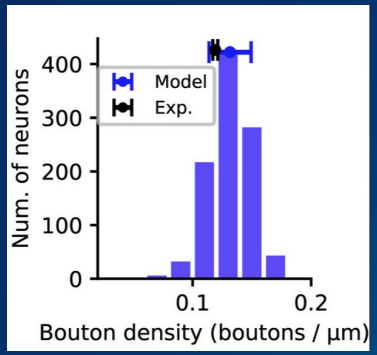

Iavarone et al., 2023

2024 human circuitry model

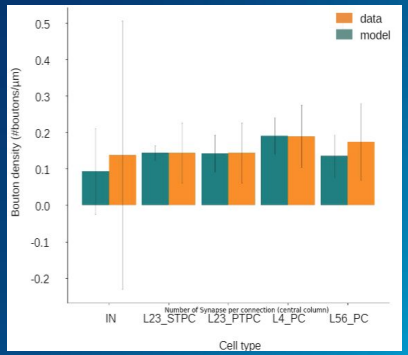

WIP: Human microcircuit model

I. Subcellular - Validation of the **distribution of inter-bouton intervals**

Level 1 | Level 2 | Level 3 | Level 4 | Level 5

This demonstrates how we do not merely artificially **enforce** bouton densities (previous page), but let them emerge in a biologically realistic way.

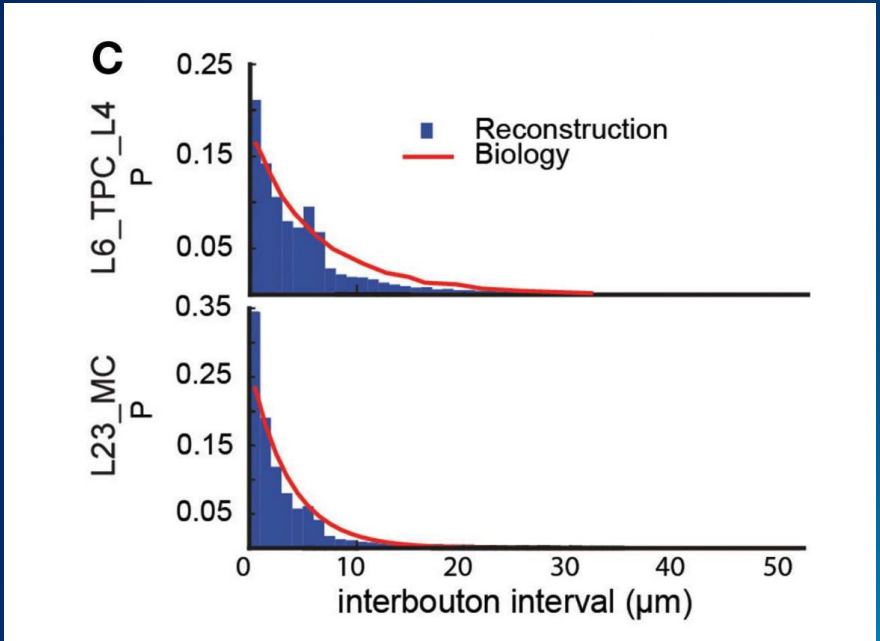

Reimann et al., 2015

I. Cellular - Validation of **dendritic morphology**

Level 1 | Level 2 | Level 3 | Level 4 | Level 5

The computational generation of dendritic morphologies accurately reproduces the anatomical properties of dendrites at cellular (A-C) and population (D) level. Both input parameters and emerging properties fit well the biological data demonstrating robustness of the synthesis algorithms.

Blue = data
Red = computational

This result is expected as the topological descriptor of dendrites is an accurate representation of the morphological characteristics of dendrites.

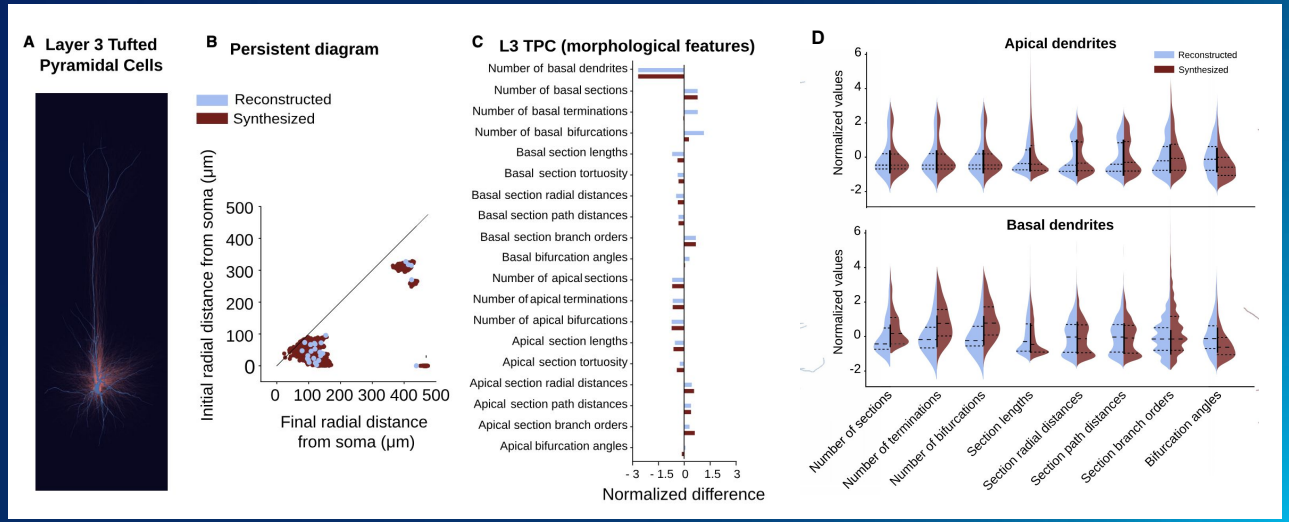

Kanari et al., 2022

I. Cellular - Validation of **dendritic physiology**

Level 1 | Level 2 | Level 3 | Level 4 | Level 5

Dendrites generated with the computational synthesis algorithm, also accurately reproduce the electrophysiological properties of neurons, even though they have not been optimized for this.

Blue = data
Red = computational

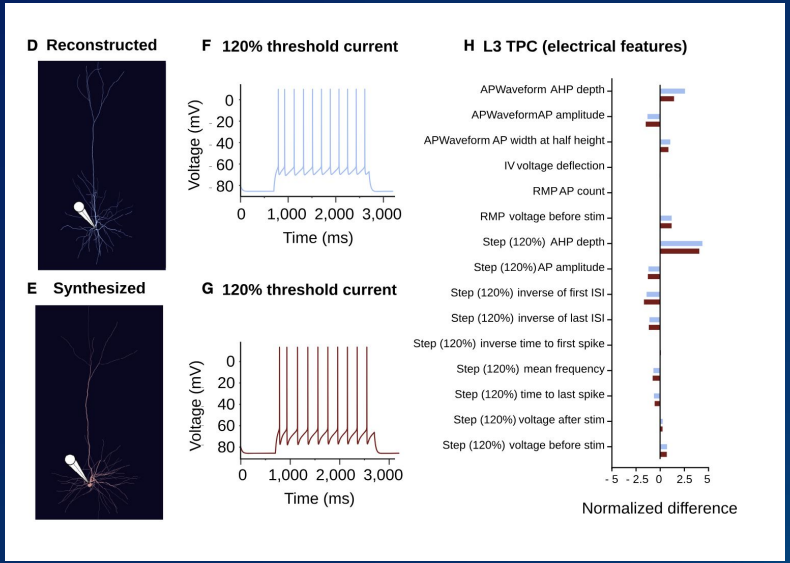

This result is highly significant as it demonstrates that the topological description of dendrites is sufficient to generate accurate electrophysiological responses.

Kanari et al., 2022

I. Cellular - Validation of **axonal morphology**

Level 1	Level 2	Level 3	Level 4	Level 5

The computational generation of axonal morphologies is an unsolved problem. We used large-scale axonal reconstructions to create an algorithm that optimizes path finding (using minimum spanning tree) and topology of axons for local branching. The generated axons that extend within and between brain regions reproduce biological properties.

Blue = data
Red = computational

These results are highly significant as it is the first computational algorithm to generate accurate axonal shapes between brain regions.

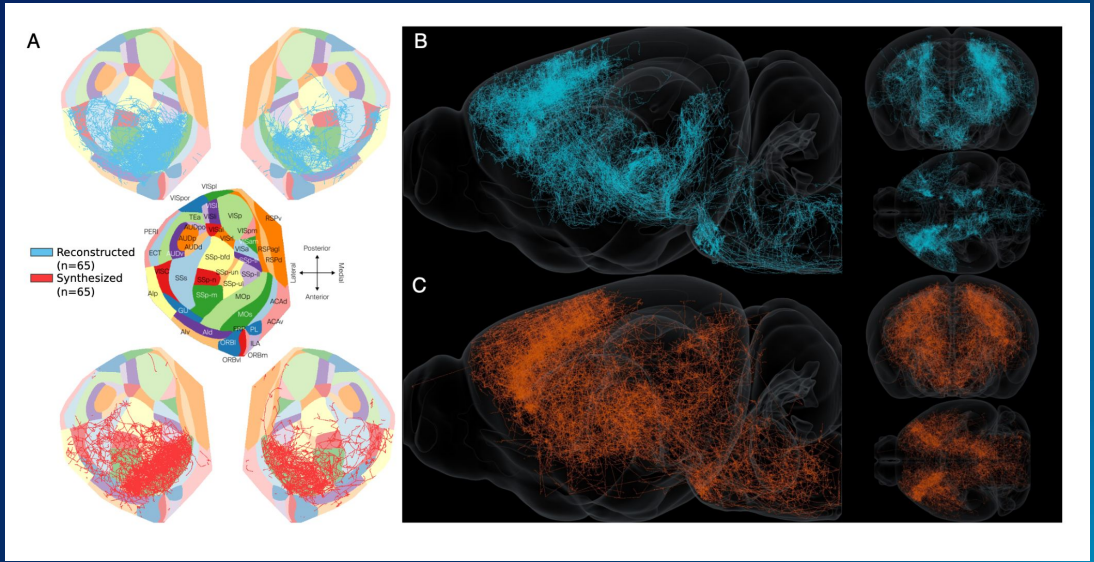

Petkantchin et al., in prep.

I. Pairwise - Validations of **synapses per connection**

Level 1 | Level 2 | Level 3 | Level 4 | Level 5

This validates the degree to which a neuron balances between forming fewer, but stronger connections with forming many but weaker ones.

2015 rat model

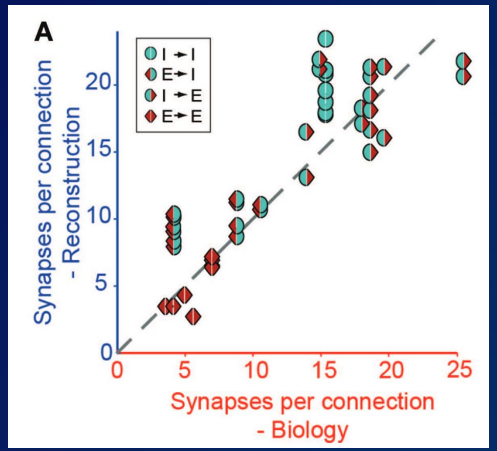

Reimann et al., 2015

We see how our techniques improve, allowing successively better fits.

2023 rat model

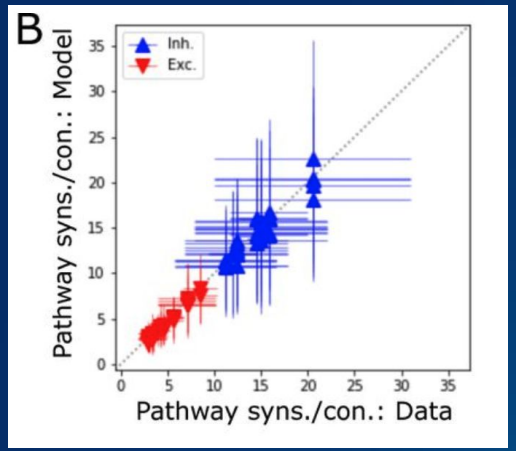

Reimann et al., 2023

2023 thalamus model

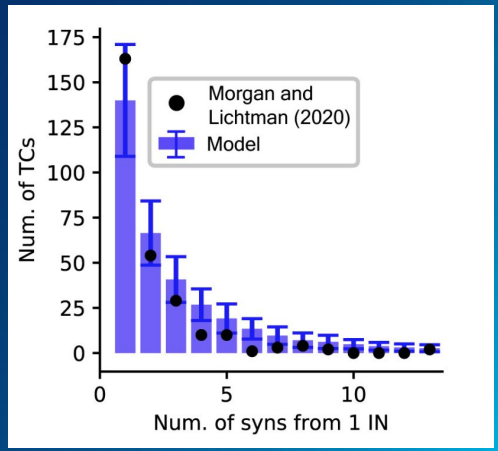

Iavarone et al., 2023

I. Pairwise - Validations of **Hippocampus connectivity**

CA3 pyramidal cell axons have collaterals, called Schaffer collaterals (SC), which heavily innervate CA1 neurons and represent their major input. In this set of analyses, we validated the anatomical properties of this innervation, in particular the synapse density across the different CA1 layers and the convergence of the SC fibers on CA1 pyramidal cells and interneurons.

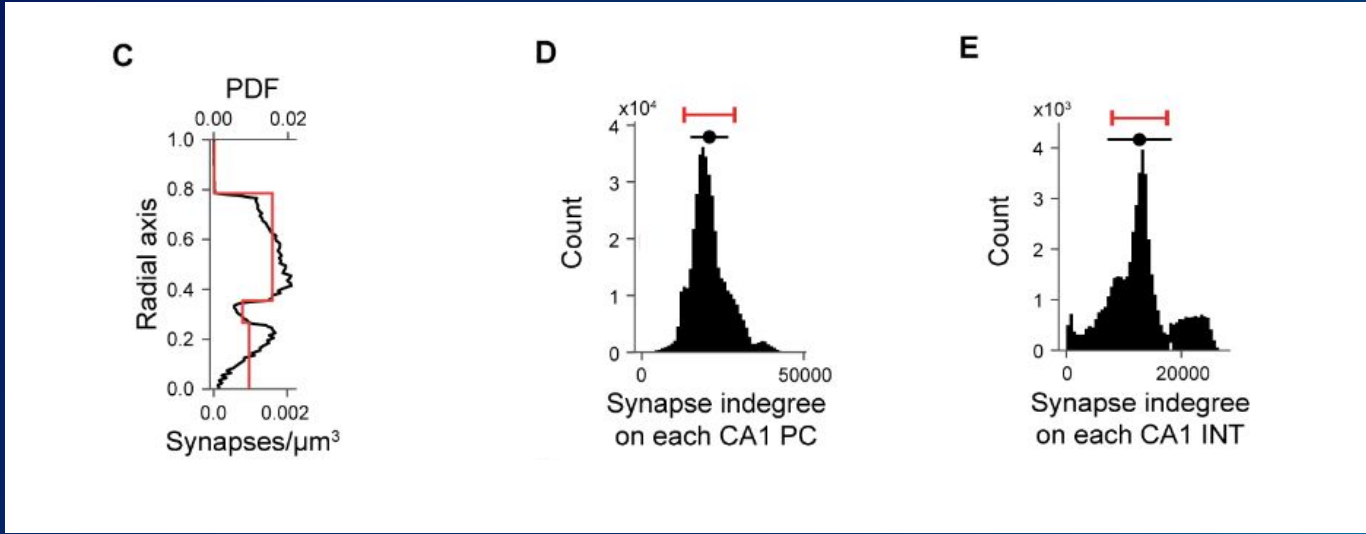

Romani et al., 2023

I. Pairwise - Validation of **gap-junction connectivity**

Level 1 | Level 2 | Level 3 | Level 4 | Level 5

Neuron in the RT nucleus of the thalamus are connected via gap-junctions. Here we compare the number of neurons connected via gap-junctions in different distance bins to a biological reference.

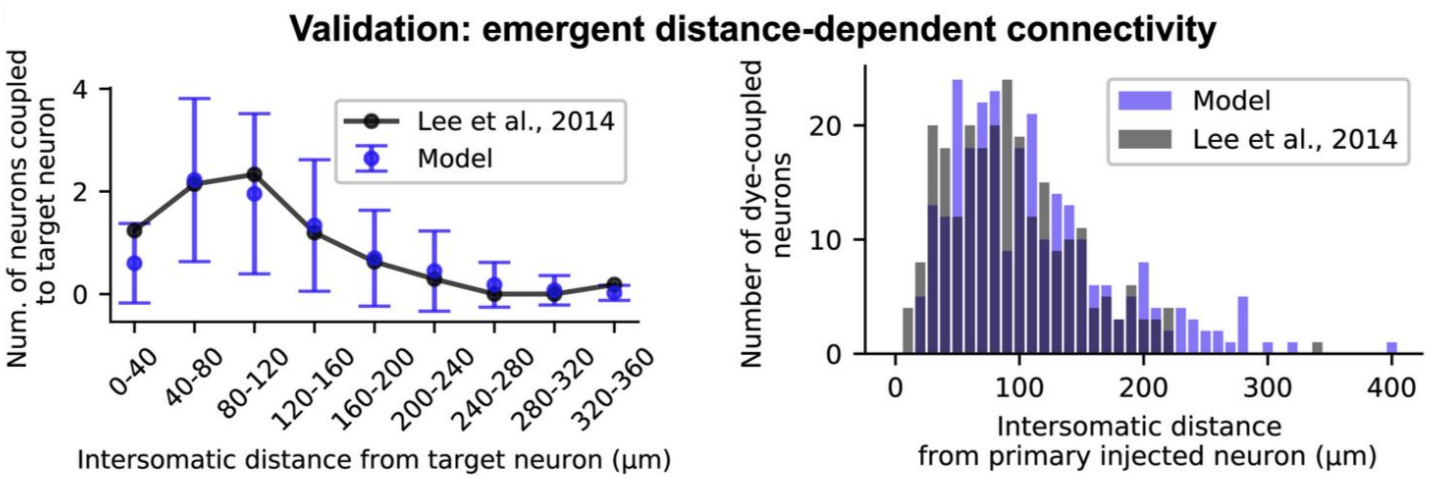

Iavarone et al., 2023

I. Population - Validation of **neuronal composition**

Level 1 | Level 2 | Level 3 | Level 4 | Level 5

This validates how much we match the overall “recipe” of a microcircuit, i.e. how much of each layer and associated neurons are present.

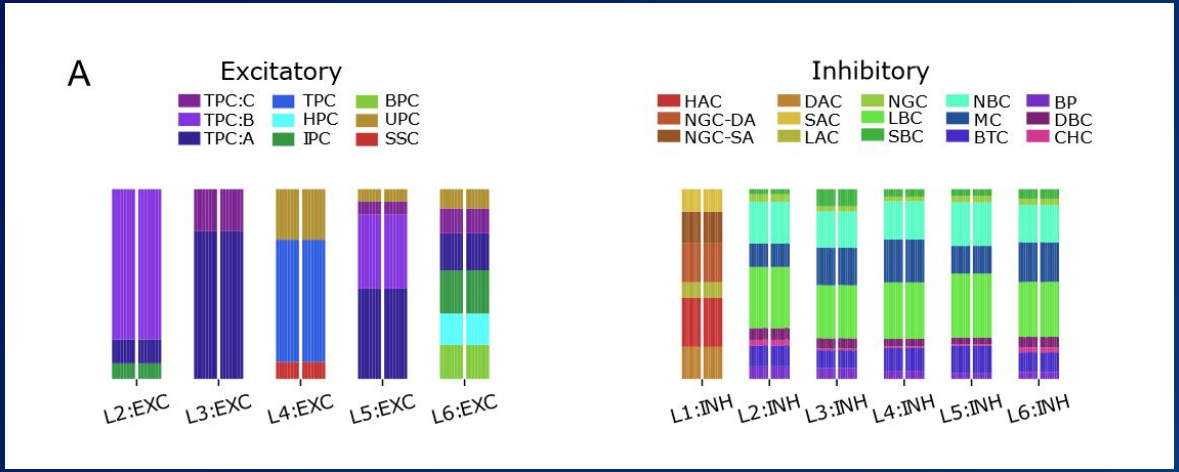

Reimann et al., 2023. In each pair of stacked histograms, the left indicates the biological data we are trying to match and the right is the model. Data is normalized, i.e. we see the relative composition per layer.

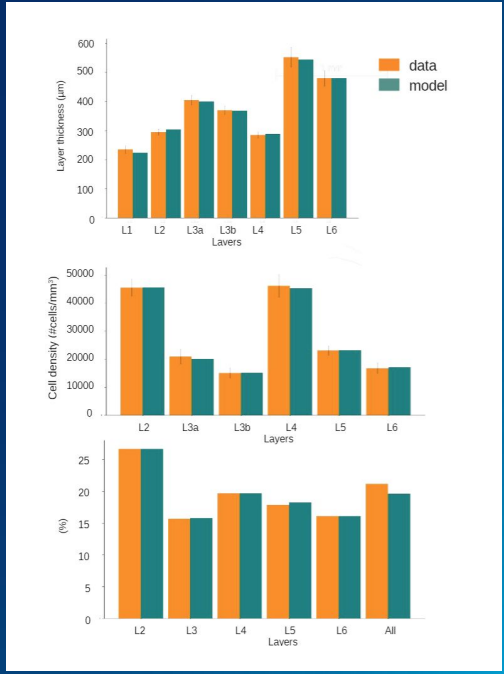

WIP: Human microcircuit model. We see absolute counts / percentages per layer.

I. Population - Qualitative validation of **neuron placement**

Level 1 | Level 2 | Level 3 | Level 4 | Level 5

This demonstrates that the neuron morphologies we place provide a good anatomical fit; their dendrites and axons reach the correct layers and do not “stick out” of the volume too much.
Note: sticking out to the left and right is no issue, as those are not true anatomical boundaries.

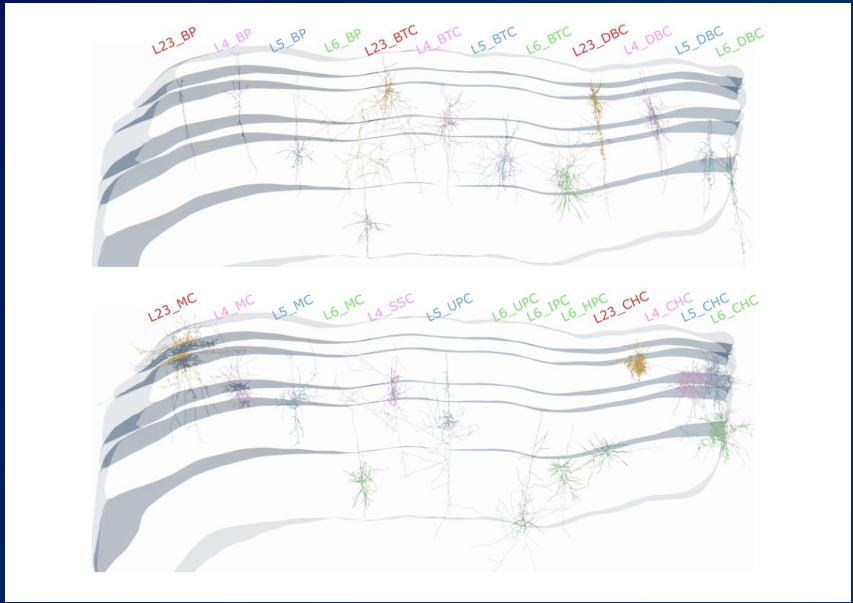

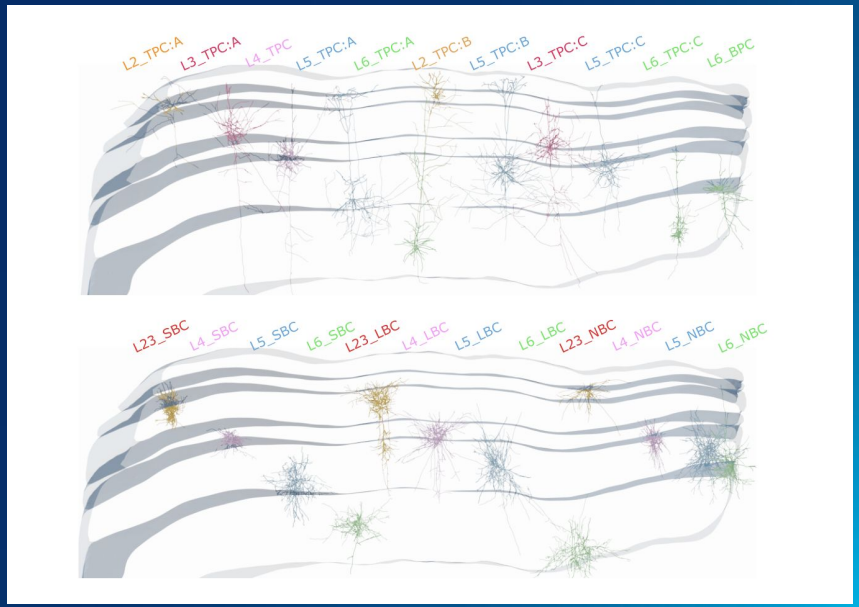

Reimann et al., 2023. Supplementary figure.

I. Population - Validation of **volume filling fractions**

Level 1 | Level 2 | Level 3 | Level 4 | Level 5

This plot shows what fraction of the grey matter space is occupied by axons and dendrites.

The logic is, if we place the right *number* of neurons with the right *morphologies* at the right *locations*, then this should emerge naturally. Specifically, we expect this to emerge for dendrites, which are known to be only local.

For axons, we expect the filling fraction to be lower in the model, to leave room for long-range axons that are not part of the model.

We find an overall qualitative agreement.

NB: the reference is only a single EM measurement, so we should not expect a perfect match.

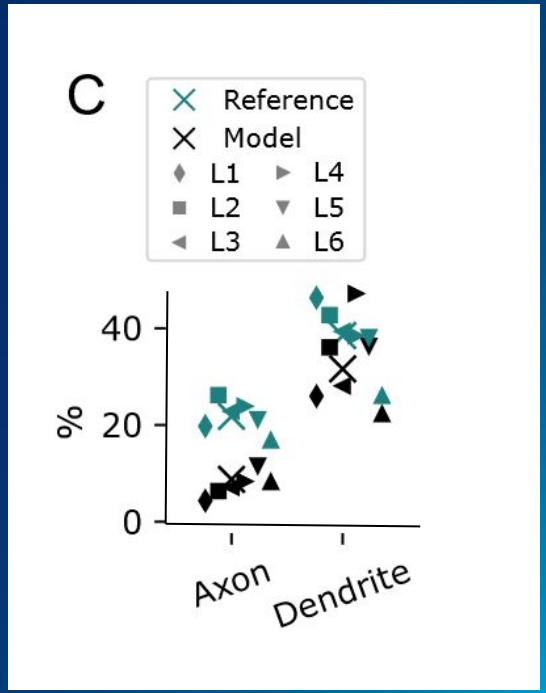

Reimann et al., 2023

I. Network - Validation of **volumetric inhibitory synapse densities**

Level 1 | Level 2 | Level 3 | Level 4 | Level 5

This plot shows the number of inhibitory synapses per cubic micrometer.

As inhibitory connections are largely local, this should emerge correctly if we place the right number of inhibitory neurons and give them the right number of connections.

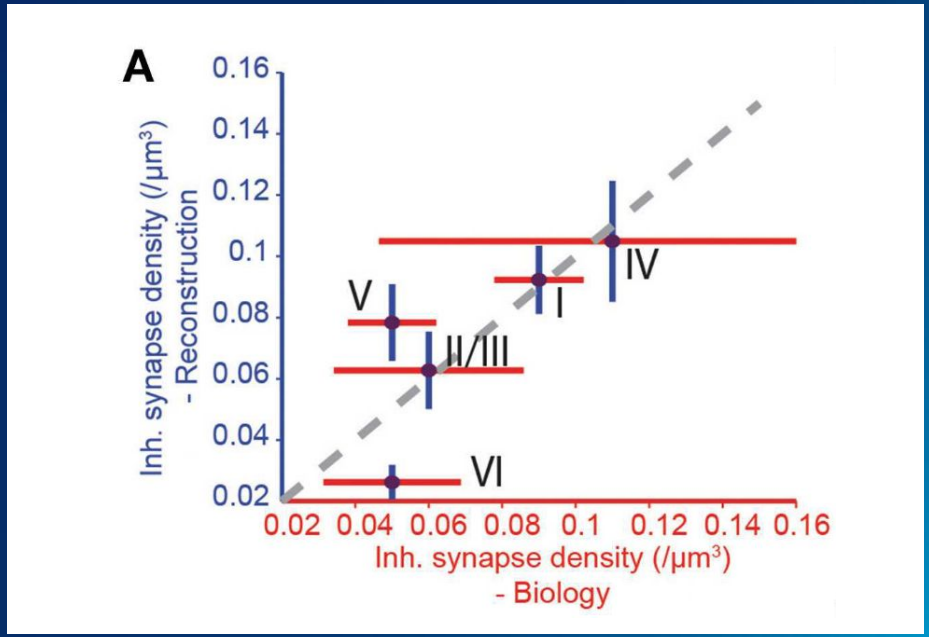

Reimann et al., 2015

I. Network - Validation of **total excitatory strength** within and between somatosensory subregions

Level 1 | Level 2 | Level 3 | Level 4 | Level 5

Unlike inhibitory connections (previous page), excitatory connections also innervate a region from further away.

This validation shows that we match the right balance between *local* and *mid-range* innervation. In (E), each point represents the volumetric excitatory synapse density from only local sources in a subregion of the model.

We find an overall match, although the biological data has a larger spread.

In (H) we see the volumetric excitatory synapse density from local and midrange sources combined.

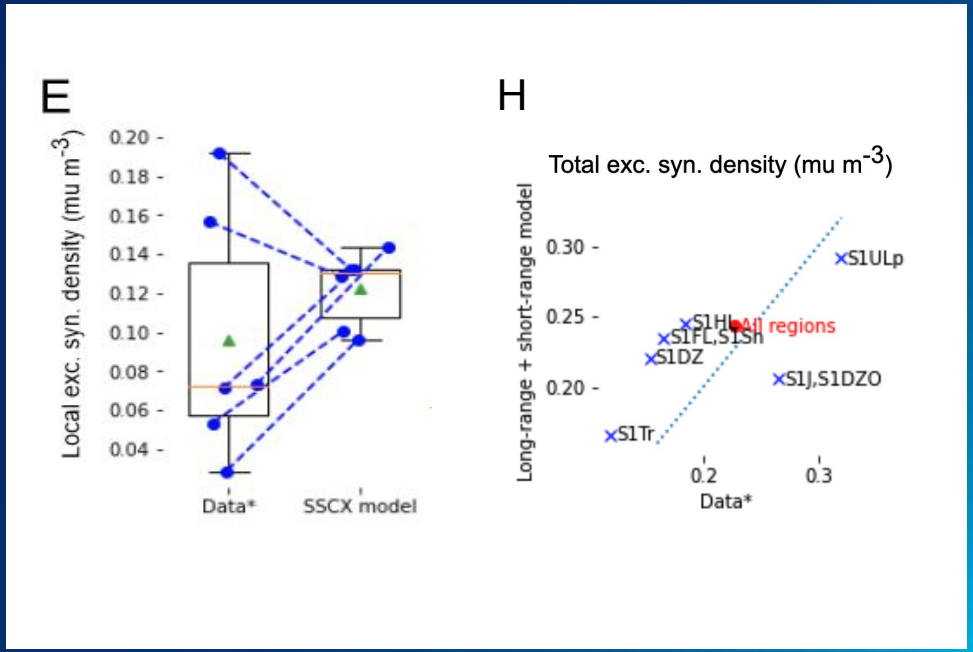

Reimann et al., 2023

I. Network - Validation of **common neighbor bias** of connectivity

The common neighbor bias is a phenomenon in cortical connectivity where a statistical dependence between connections is observed that cannot be captured by simplified models of connectivity. We call each neuron connected to another its *neighbor* and a *common neighbor* of a pair of neurons is one that is connected to both.

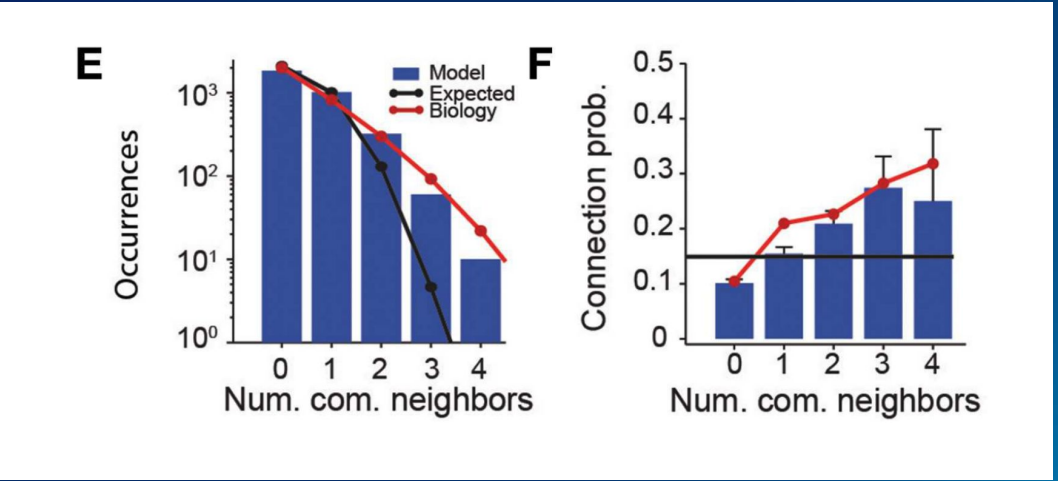

Reimann et al., 2015

We observe that the number of common neighbors is higher than expected from the overall level of connectivity (E). Specifically, connections are more likely between pairs of neurons with many common neighbors (F). This leads to a form of connectivity clustering.

I. Network - Validation of **simplex overexpression**

Clustering of connections (previous page) leads to the formation of large, tightly connected motifs called *directed simplices*. We see that they are overexpressed in many connectomes from worm to mouse, and equally so in our model. Additionally, reciprocal connections are more likely to occur in large simplices.

Solid lines = data

Dashed = control models of connectivity

- Configuration Model (preserving neuron degrees)
- Erdos-Renyi (completely random)
- Distance-dependent
- Underlying undirected graph preserved
- Reciprocal connections shuffled

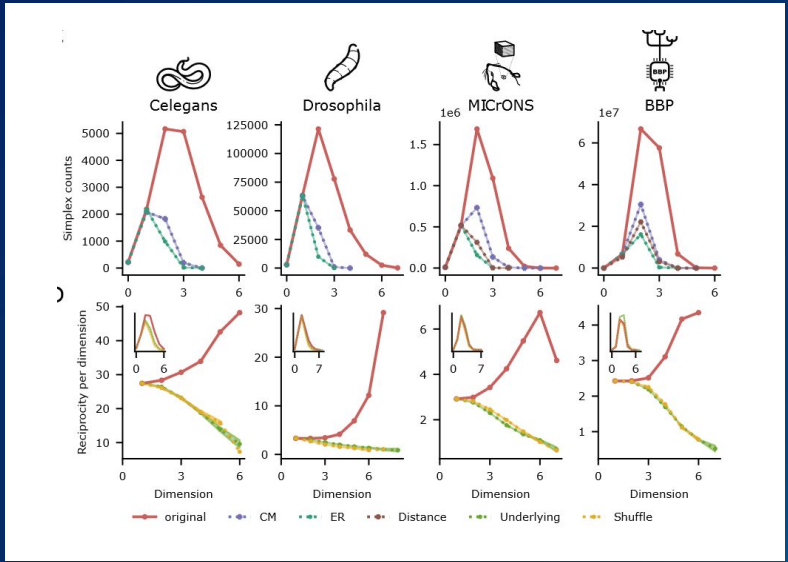

These results are highly significant as it is an unsolved problem in mathematics to generate networks with these properties!

Egas-Santander et al., 2024

I. Network - Validation of **layer profiles** of long range inputs

We built a parametric model of the anatomy of long-range connectivity in mouse cortex.
As part of this, we predict the laminar profiles of synapse densities from the various projections.
Here, we compare our predictions to a reference given by the whole-brain connectome of the Allen Institute.

We see that the error in most cases is below two standard deviations of the biological data.

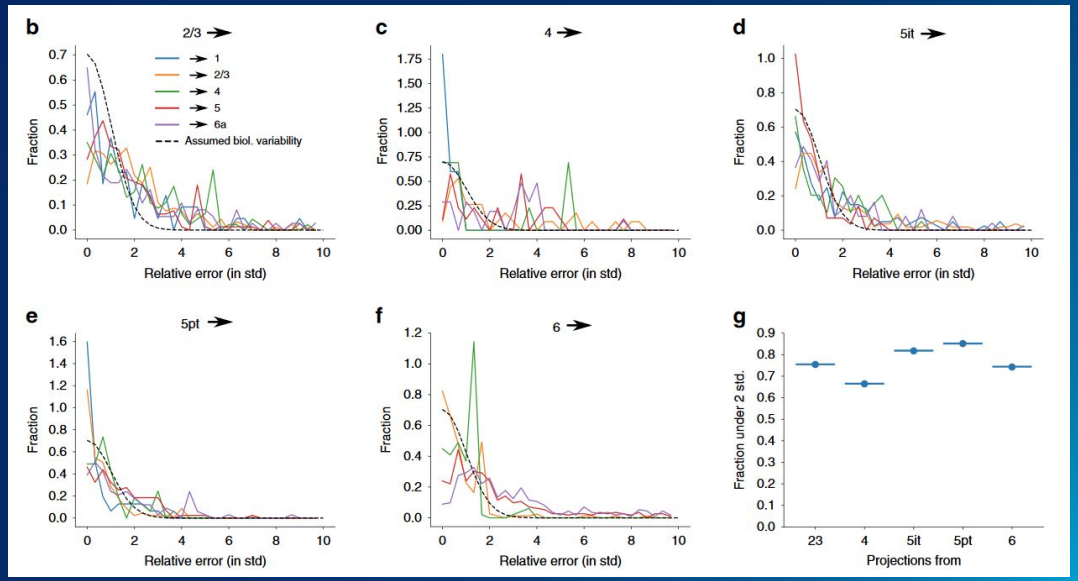

I. Network - Validation of the **topography of inter-regional connectivity**

Level 1 | **Level 2** | Level 3 | Level 4 | Level 5

We also provide a parameterized version of predicted **topography** of inter-regional connectivity, which we validate here for the visual system.

In the plot, similarly colored parts connect predominantly to each other.
Left: The center shows the reference of the Allen Institute connectome, the surrounding plots our parametric version.

Right: The topographical mapping from VISp is a result of linear transformations.
We compare our version to two references.

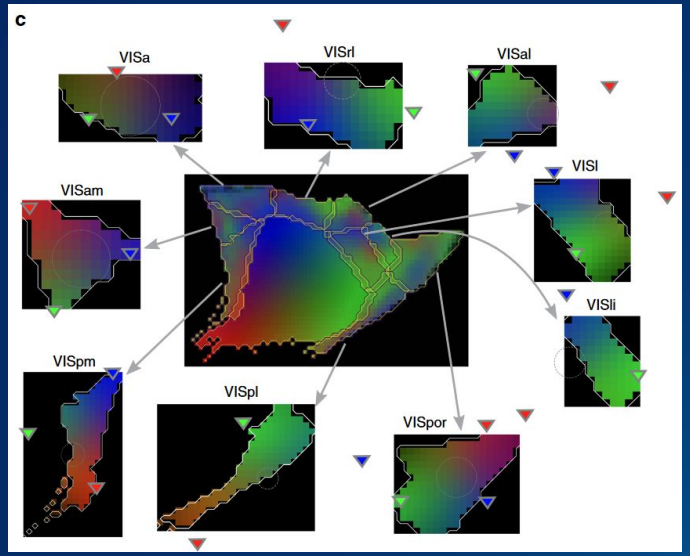

Table 1 Validation of predicted mapping

		Wang and Burkhalter[29]	Juavinett et al.[30]	Our mapping
VISpl	*reflection?*	Yes	Yes	Yes
	rotation?	90 °	n/a	90 °
VISpor	*reflection?*	None	None	None
	rotation?	180 °	n/a	180 °
VISl	*reflection?*	Yes	Yes	Yes
	rotation?	None	n/a	None
VISli	*reflection?*	None	None	None
	rotation?	None	n/a	None
VISal	*reflection?*	None	None	None
	rotation?	180 °	n/a	180 °
VISrl	*reflection?*	Yes	Yes	Yes
	rotation	None	n/a	None
VISa	*reflection?*	None	n/a	None
	rotation?	90 °	n/a	90 °
VISam	*reflection?*	None	None	None
	rotation?	90 °	n/a	90 °
VISpm	*reflection?*	Yes	Yes	Yes
	rotation?	None	n/a	None

Comparing linear transformations from source to target coordinate system in our results to the ones of Wang and Burkhalter[29] and Juavinett et al.[30], n/a indicates that a paper provides no data on a transformation

I. Network - Validation of **combinations of regional targets**

A long-range projecting neuron can innervate several neighboring regions at once. However, the combinations that are innervated together are not chosen randomly. Here we validate our model of the process.

Left: Distributions of the number of visual areas innervated together by individual VISp neurons.

Top: Reference
Bottom (dashed box): Model
Outside dashed box: Predictions for other source layers.

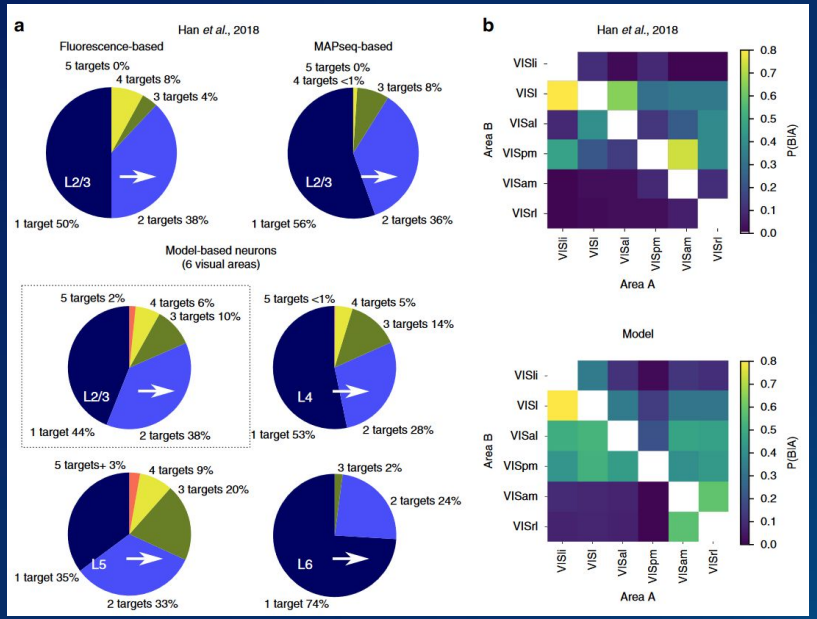

Right: Overview of which regions are innervated together more often than expected (yellow) and which ones less often than expected (blue).

Top: Reference
Bottom: Model

I. Network - Validation of **dendritic connectivity**

Level 1 | Level 2 | Level 3 | Level 4 | Level 5

Dendrites generated with the computational synthesis algorithm, also accurately reproduce the connectivity between neurons, even though they have not been optimized for this. The accurate connectivity emerges from the correct modeling of dendritic shapes.

This result is highly significant as it demonstrates that the topological description of dendrites is sufficient to generate accurate connectivity between neurons.

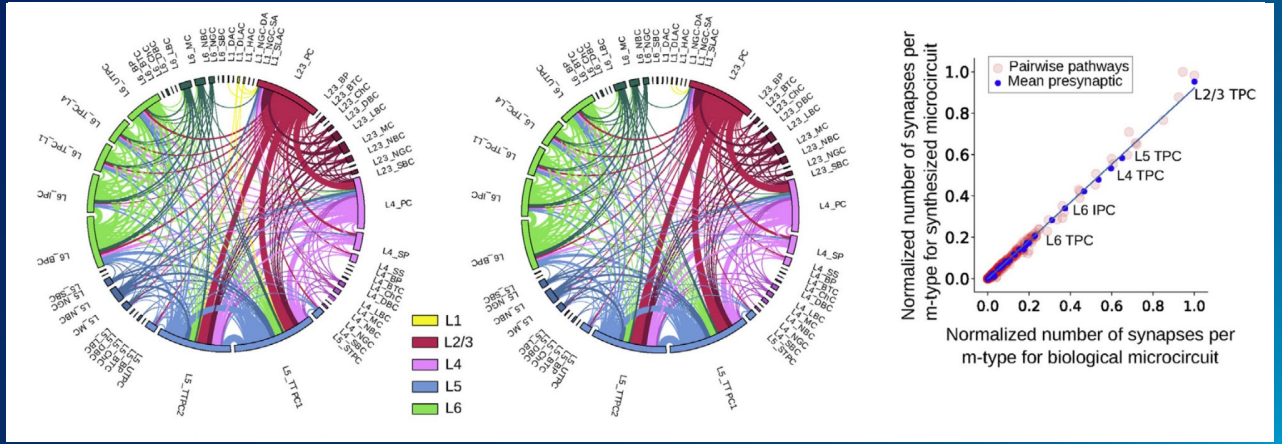

Kanari et al., 2022

I. Network - Validation of **axonal connectivity**

Level 1 | Level 2 | Level 3 | Level 4 | Level 5

Axons generated with the computational synthesis algorithm also accurately reproduce the connectivity between neurons, even though they have not been optimized for this. The long-range connectivity emerges from the correct modeling of axonal shapes and accurately links brain regions at brain-wide scale.

A - C: model
D. blue: data; red: model

These results are highly significant as it is an unsolved problem to generate networks that are biologically accurate at different computational scales (from single cells to inter-regional connectivity).

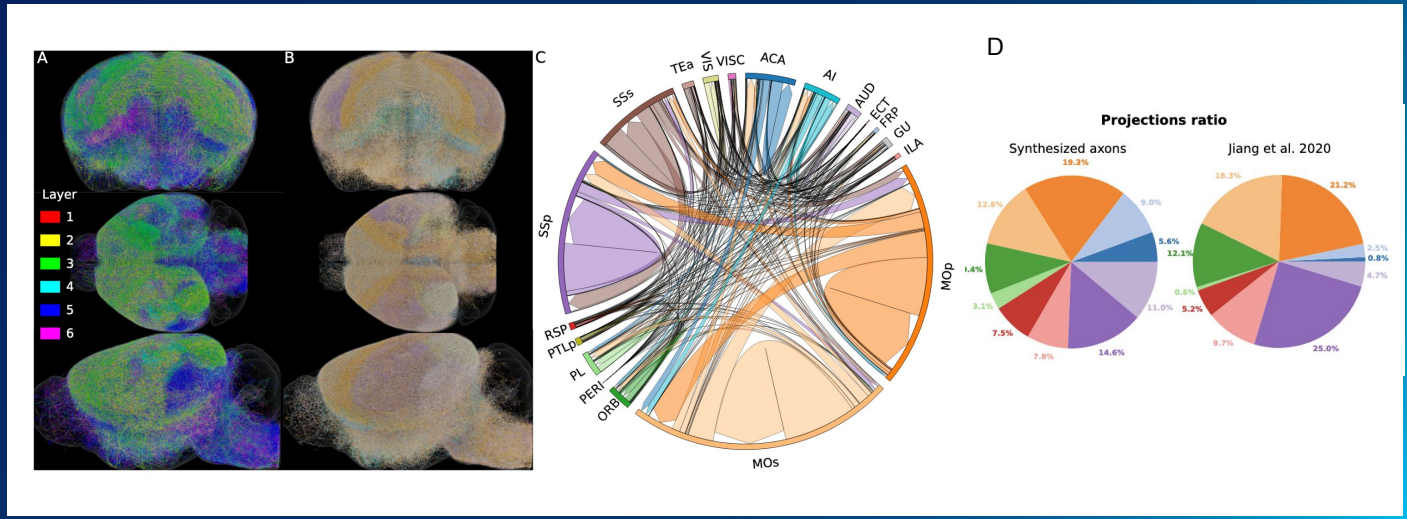

Petkantchin et al., in prep.

Biological Comparison - Structural and Functional Validations

I. Structural validations - small to large scale
   A. Subcellular
   B. Pairwise
   C. Population
   D. Network

II. Functional validations - small to large scale
   A. Single cell
   B. Paired cells
   C. Population

III. References

II. **Single cell -** Validation of **single cell electrical models**

Level 1 | **Level 2** | Level 3 | Level 4 | Level 5

The features of somatic voltage traces that are used to fit single cell electrical models are validated against the variability of the biological recordings.

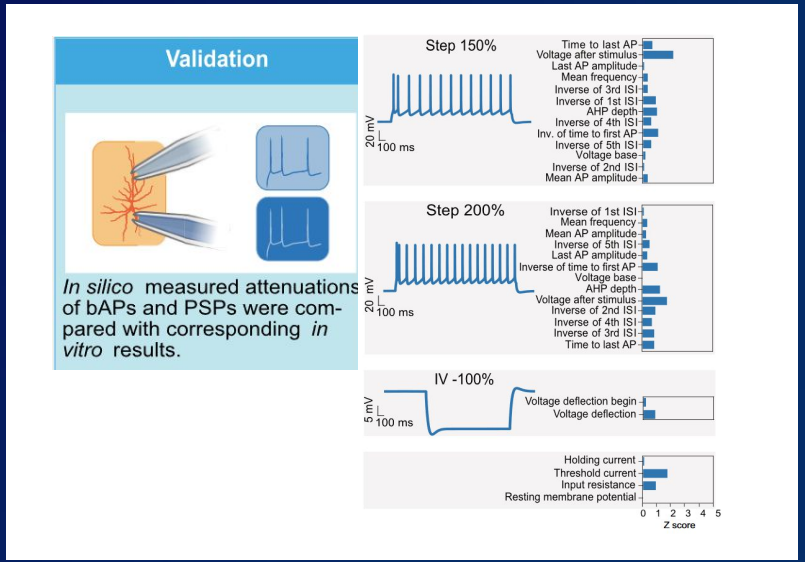

Reva et al., 2023

Level 1 | Level 2 | **Level 3** | Level 4 | Level 5

The attenuation of EPSPs and the action potential are not fitted, but emerge.

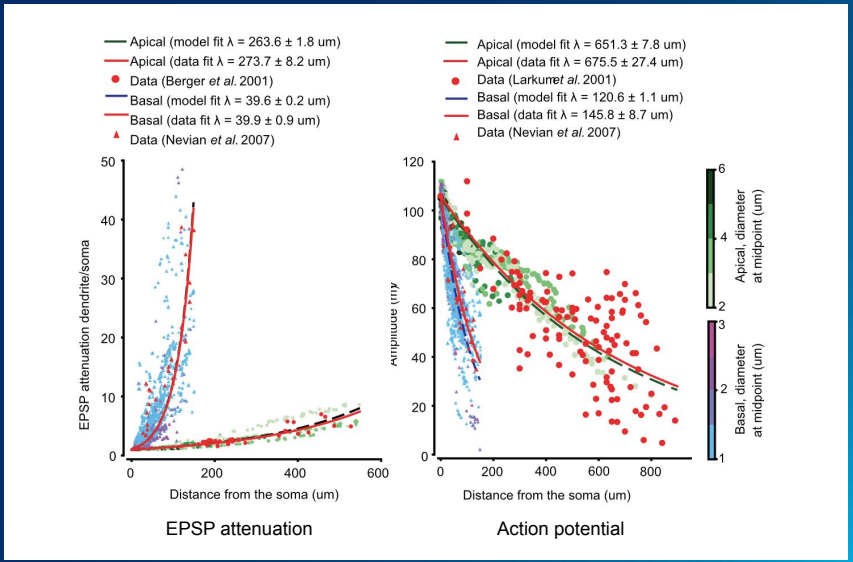

Reva et al., 2023

II. **Paired -** Validations of **PSP amplitudes**

Level 1 | **Level 2** | Level 3 | Level 4 | Level 5

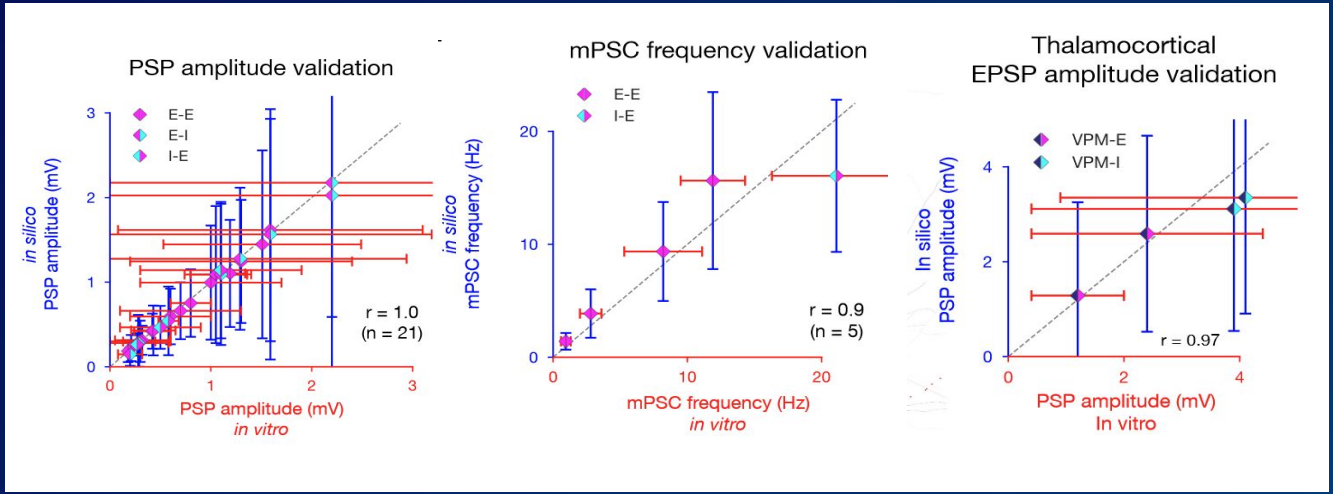

Isbister et al., 2023

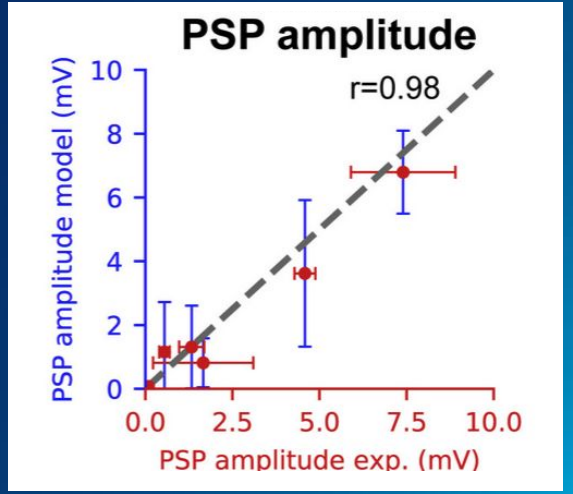

Iavarone et al., 2023

II. **Paired -** Validation of **connection physiology**

Level 1 | **Level 2** | Level 3 | Level 4 | Level 5

After the anatomical properties of the Schaffer collaterals (SC) have been constrained and validated, we looked at the electrical properties. Here we compare the PSP of SC on pyramidal cells and two classes of interneuron, cannabinoid receptor type 1 positive and negative.

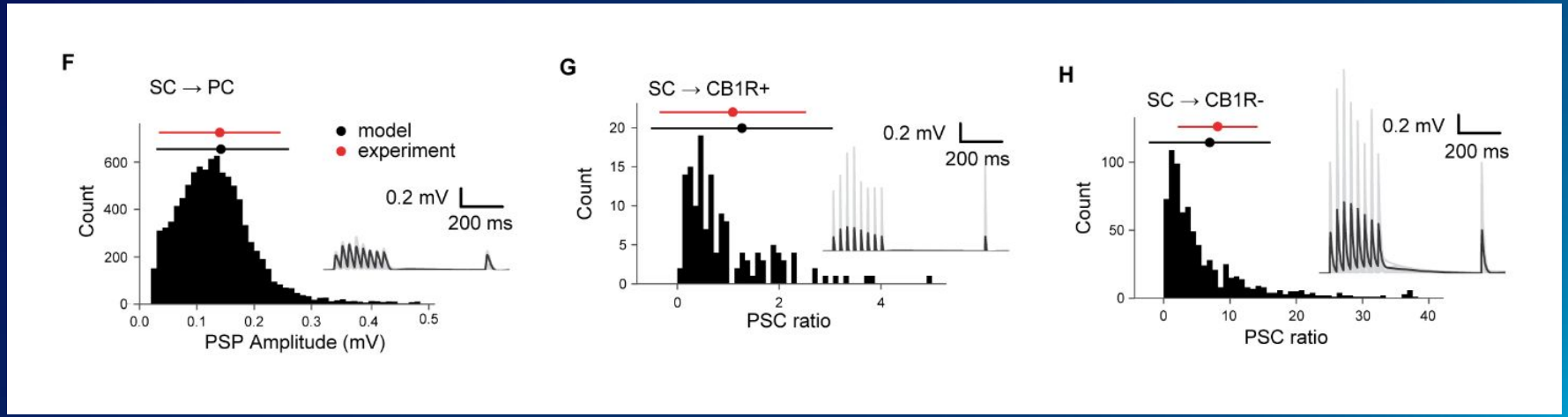

Romani et al., 2023

II. **Paired -** Validations of **PSP variability**

Synaptic connections are noisy, because the transmission often fails. The amount of noise can be reduced by forming connections that have multiple independent release sites. The added redundancy will reduce the relative amount of noise. Here we show that we simultaneously match the strength and variability of synaptic connections. Something that is enabled by the biological detail added.

First panel shows our matching the variability in a pathway that is explicitly fit to the data (level 2).

Far right panel shows this emerging in various other pathways (level 3).

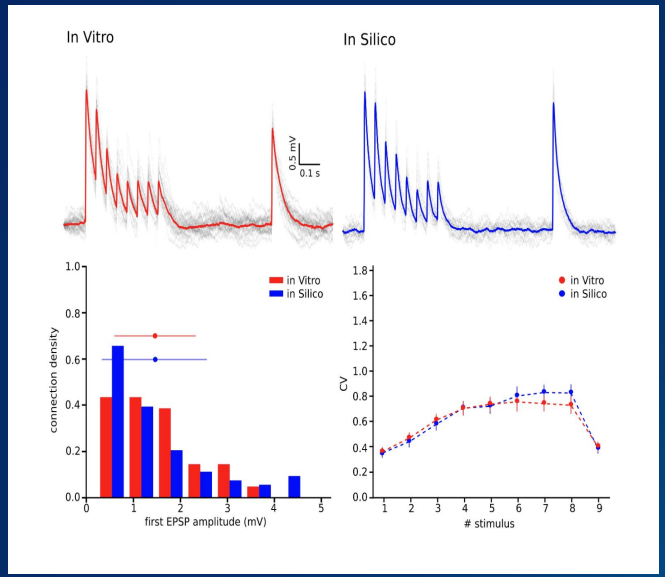

Barros-Zulaica et al., 2019

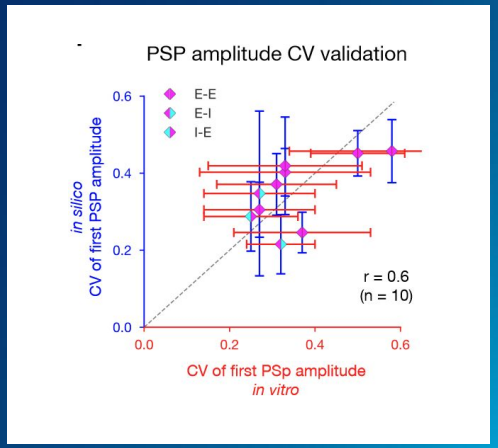

Isbister et al., 2023

II. **Paired -** Validation of **STDP profiles**

Level 1 | Level 2 | Level 3 | Level 4 | Level 5

This is a validation of calcium-based plasticity simulations implemented in the model. Plasticity parameters were fit to the data points with the black arrows. All others then emerge. This is highly remarkable as myriad aspects of the model, from subcellular to anatomical and physiological, must be correct for this to emerge.

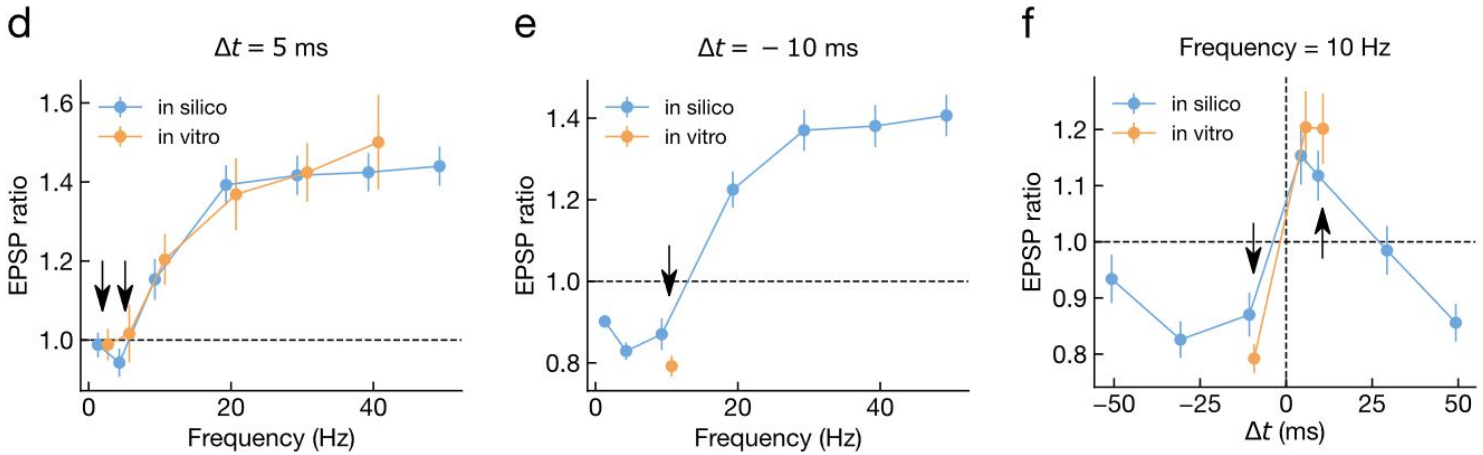

II. Population - Validation of **spontaneous firing rate ratios**

Level 1 | **Level 2** | Level 3 | **Level 4** | Level 5

We aim to provide dynamic states at different levels of excitability that still preserve the ratios between firing rates of different populations. On the left, we show that the ratios are preserved at all levels of excitability.

The levels of excitability are determined by the strengths of excitatory inputs into the neurons that represent the missing extrinsic inputs from outside the modeled volume. Consequently, we expect the strengths to be determined by the amount of missing extrinsic inputs, which we can estimate from the density of excitatory inputs on dendrites.

We find that they are indeed strongly correlated.

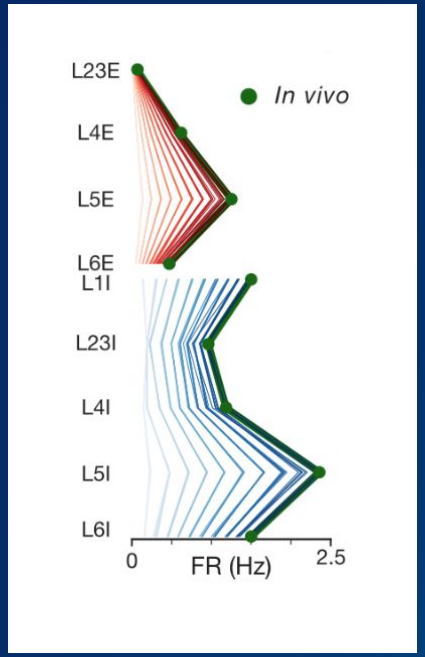

Isbister et al., 2023

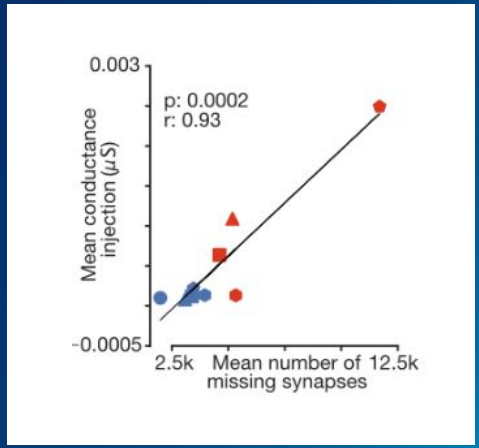

Isbister et al., 2023

II. Population - Validation of **evoked responses**

We compare the time course of responses to brief thalamic inputs to reference data. We found a good quantitative match to data from an experiment using passive whisker deflection. (Only exception is an additional 1 ms delay for inhibitory neurons in L4.)

Note: We do not match the data for active touch, which is expected as that phenomenon includes interactions between somatosensory and motor regions which our model does not include.

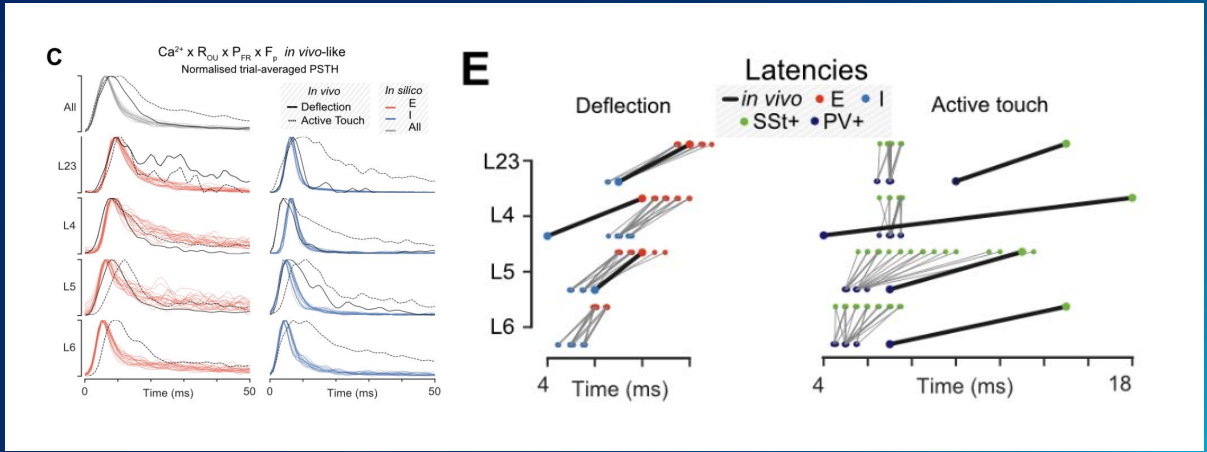

Isbister et al., 2023

II. Population - Validation of **evoked spike sequences**

Level 1 | Level 2 | Level 3 | Level 4 | Level 5

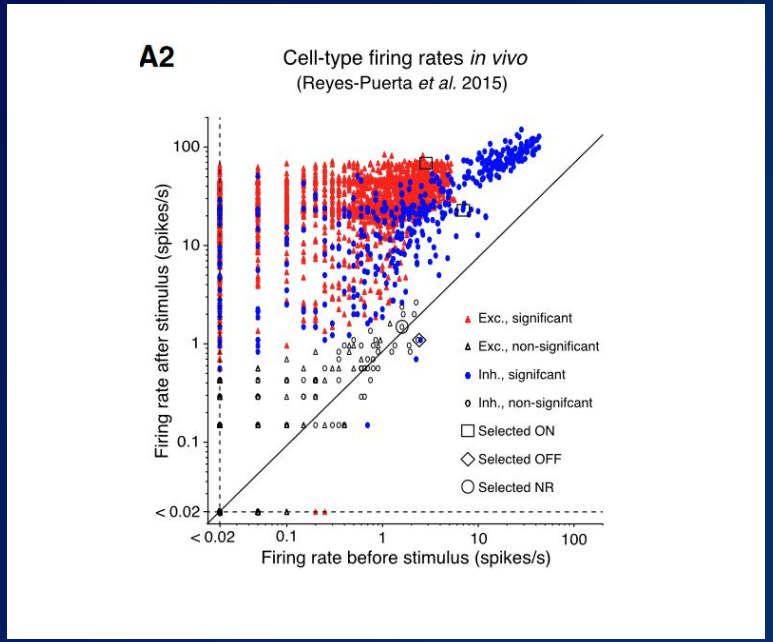

Markram et al., 2015

VS.

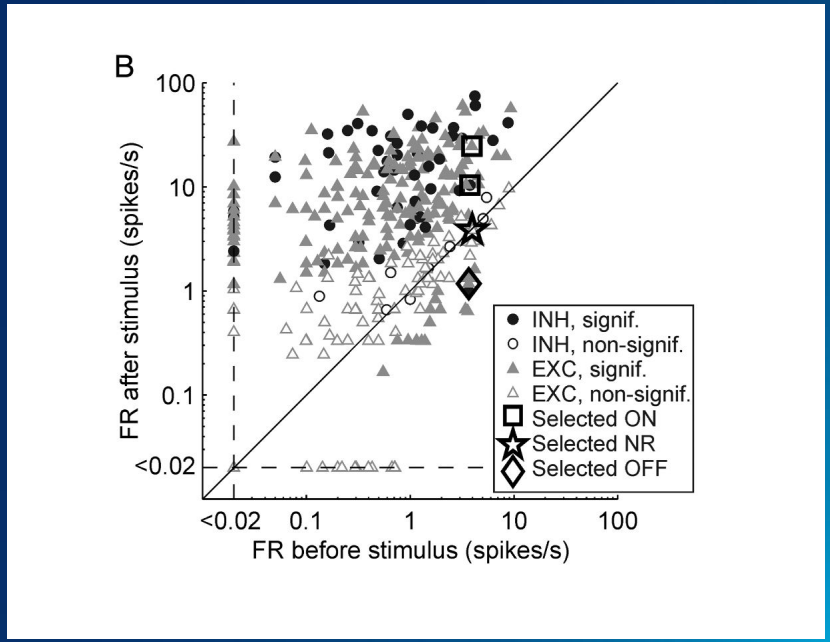

Reyes-Puerta et al., 2015

II. Population - Validation of **population coupling**

Level 1 | Level 2 | Level 3 | Level 4 | Level 5

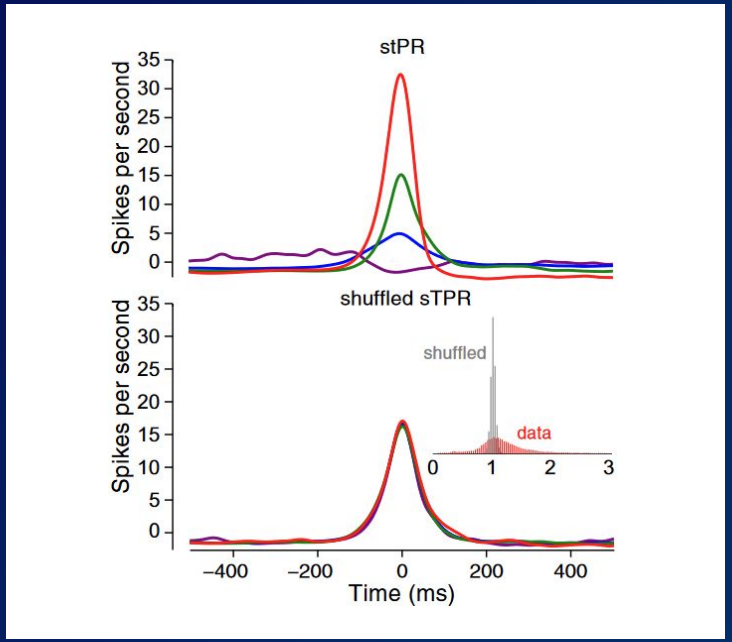

Markram et al., 2015

VS.

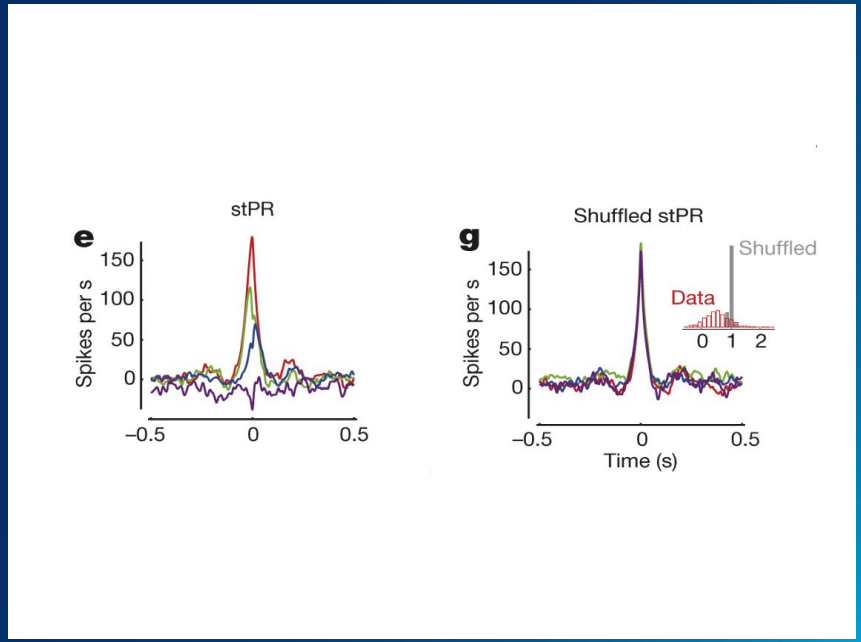

Okun et al., 2015

II. Population - Validation of **extracellularly detected firing rates** (1/2)

Level 1 | Level 2 | Level 3 | Level 4 | Level 5

In experiments, population firing rates and their distributions are detected through spike sorting of extracellular traces.

We recreate that process in simulation and validate that the resulting distributions match.

Biological reference
Simulation of spontaneous activity
Simulation of evoked activity
Earlier reference that tried to do something similar

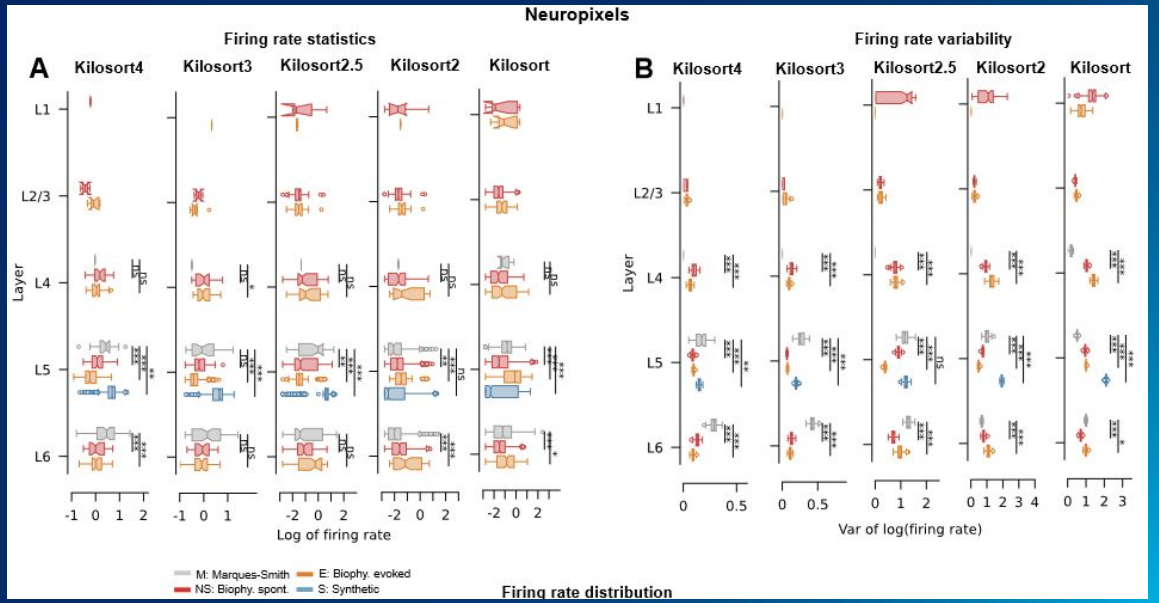

Laquitaine et al., in prep.

II. Population - Validation of **extracellularly detected firing rates** (2/2)

Level 1 | Level 2 | Level 3 | Level 4 | Level 5

In experiments, population firing rates and their distributions are detected through spike sorting of extracellular traces.

We recreate that process in simulation and validate that the resulting distributions match.

Biological reference
Simulation of spontaneous activity
Simulation of evoked activity
Earlier reference that tried to do something similar

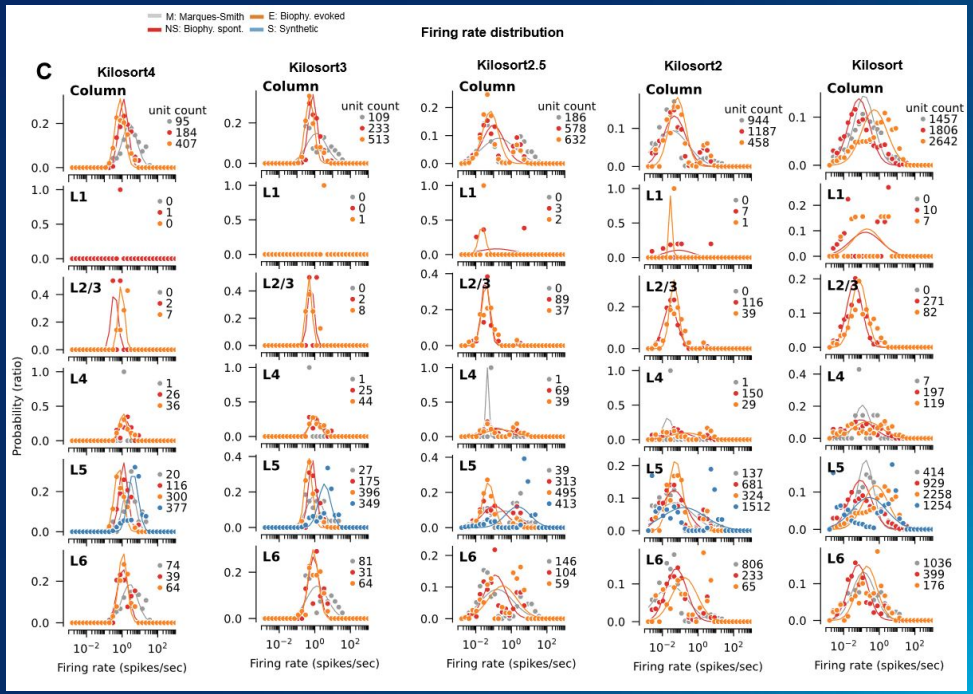

Laquitaine et al., in prep.

II. Population - Validation of the **EEG signal**

Placing the model inside a model of a rat skull, we can simulate the EEG signal with unprecedented accuracy.

The signal in response to a whisker flick matches biology.

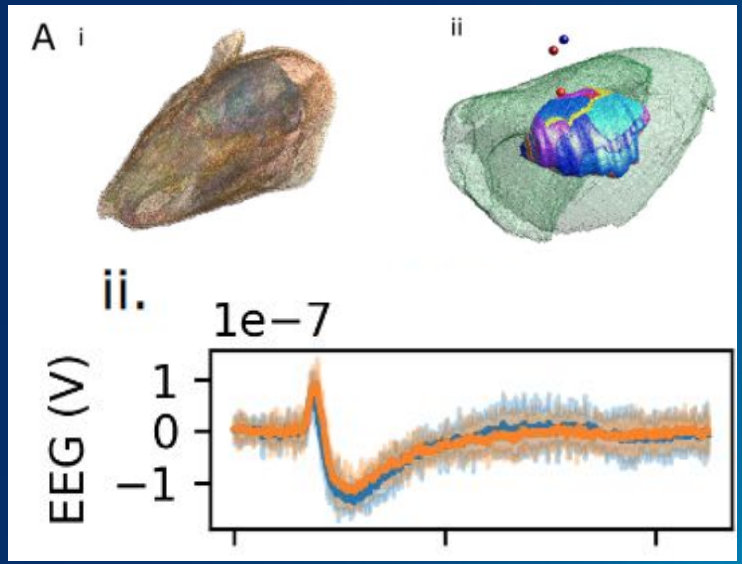

Tharayil et al., in prep.

II. Population - Validation of **structure-function relation**

Level 1 | Level 2 | Level 3 | Level 4 | Level 5

One of the most complicated questions in neuroscience is the structure-function relation: How the intricate structures formed by biological neuronal networks inform their function. We made several predictions using the model that were subsequently confirmed in biological data.

We predict that neurons that are part of the topologically most complex networks (purple) are firing more reliably than neurons in less complex networks (green); this is confirmed in experiments combining recordings with electron microscopy (“MICrONS”).

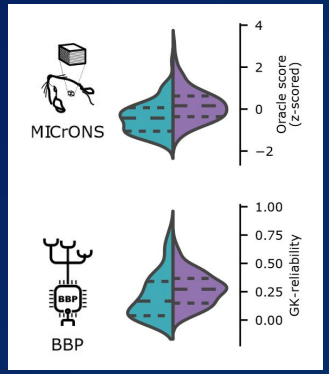

Egas-Santander et al., 2024

We predict that neurons participating in larger (“dimension”) motifs are more correlated with the overall population than expected, and that this is further influenced by their position in the motif (colors). This is also confirmed.

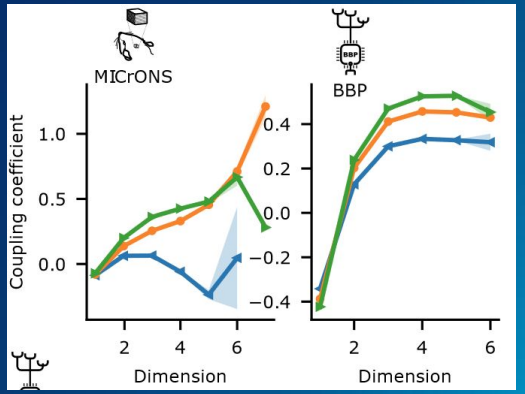

Egas-Santander et al., 2024

NB: It is **highly significant we match the overall trend** even if the exact shape of the curves differs.

II. Population - Validation of **population-level plasticity**

Level 1 | Level 2 | Level 3 | Level 4 | Level 5

Plasticity with biophysical detail has so far been almost exclusively studied at the pairwise level. Here, we made a novel prediction about how it plays out at the population level that has subsequently been validated in biological data (neuron recordings, followed by electron-microscopic reconstruction).

We predict that central connections, i.e. connections that participate in many dense motifs, are favored by plasticity and end up functionally stronger.

This is confirmed in the MICrONS data.

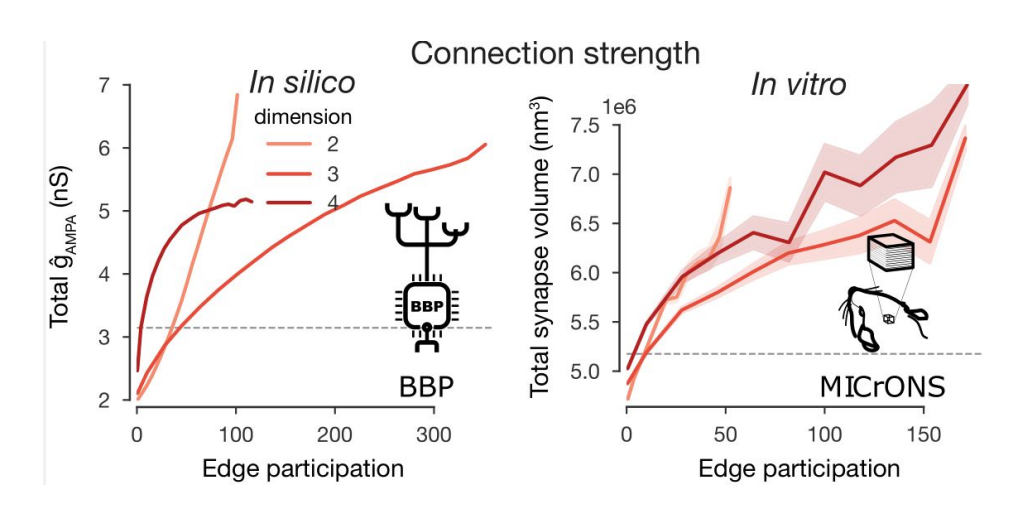

Ecker et al., 2024

III. References

- Reimann et al., 2015 - https://doi.org/10.3389/fncom.2015.00120
- Barros-Zulaica et al., 2019 - https://doi.org/10.3389/fnsyn.2019.00029
- Chindemi et al., 2022 - https://www.nature.com/articles/s41467-022-30214-w
- Kanari et al., 2022 - https://doi.org/10.1016/j.celrep.2022.110586
- Reimann et al., 2023 - https://www.biorxiv.org/content/10.1101/2022.08.11.503144v4.abstract
- Reva et al., 2023 - https://www.cell.com/patterns/fulltext/S2666-3899(23)00239-8
- Romani et al. 2023 - http://biorxiv.org/lookup/doi/10.1101/2023.05.17.541167
- Isbister et al., 2023 - https://www.biorxiv.org/content/10.1101/2023.05.17.541168v5
- Iavarone et al., 2023 - https://www.sciencedirect.com/science/article/pii/S2211124723002115
- Egas-Santander et al., 2024 - https://www.biorxiv.org/content/10.1101/2024.03.15.585196v3
- Ecker et al., 2024 - https://www.biorxiv.org/content/10.1101/2023.08.07.552264v5
- Laquitaine et al., in prep. - Contact Steeve Laquitaine
- Tharayil et al., in prep. - Contact Joseph Tharayil
- WIP human model - Contact Natali Barros-Zulaica
- Petkantchin et al. in prep. - Contact Remy Petkantchin

Thank you!

www.epfl.ch/research/domains/bluebrain

Published Oct. 2024